Expression of Chick *Fgf19* and Mouse *Fgf15* Orthologs Is Regulated in the Developing Brain by *Fgf8* and *Shh*

L. Gimeno[†] and S. Martinez[*]

Fibroblast growth factors (Fgfs) constitute a family of signaling molecules that play essential roles in development. We have studied the expression pattern of mouse *Fgf15* in the developing brain. *Fgf19* is another member of the FGF family that has been suggested as the chick and human ortholog of mouse and rat *Fgf15*. Here, we compare the expression pattern during neural development of chick *Fgf19* with mouse *Fgf15*. Unlike *Fgf15*, *Fgf19* presents an expression in the isthmic alar plate, diencephalic and mesencephalic parabasal plates, hindbrain basal plate, as well as in the zona limitans intrathalamica (zli). Moreover, we explored the regulation between *Fgf19* and the signaling molecules of the isthmic and zli organizers: *Fgf8* and *Shh*, respectively. Considering the possibility that *Fgf19* plays a similar role in humans and chicks, this finding could explain the significant diencephalic phenotypic differences between humans and mice in models and diseases where the Shh pathway is affected. *Developmental Dynamics 236:2285–2297, 2007.*

Key words: fibroblast growth factor; Fgf; Fgf15; Fgf19; Fgf8; Shh; neural tube; neural development; secondary organizers; central nervous system

Accepted 23 May 2007

INTRODUCTION

Neural tube segmentation and regionalization are complex developmental processes controlled by the expression of a variety of developmental genes, which include transcription factors and secreted signaling molecules (Shimamura et al., 1995; Shimamura and Rubenstein, 1997; Rubenstein et al., 1998). Fibroblast growth factors (Fgfs) form a family of polypeptides that can activate fibroblast proliferation and epithelial cell growth (Armelin, 1973), as well as play essential roles as secreted signaling molecules in development, affecting cell proliferation, differentiation, and survival. Moreover,

ABBREVIATIONS AER apical ectoderm ridge **bp** branchial pouch **CB** cerebellum **cp** choroidal plexus **D** diencephalon **F** forebrain **Fgf** fibroblast growth factor **Hb** hindbrain **Hy** hypothalamus **IIIm** oculomotor nerve **Is** isthmus **IsO** isthmic organizer **IVm** trochlear nerve **M** mesencephalon **mXII** hypoglossal nucleus **os** optic stalk **ot** optic tectum **otv** otic vesicle **ov** optic vesicle **PCL** Purkinje cell layer **Pt** pretectum **Pth** prethalamus **r1–7** rhombomeres 1–7 **rbl** rombic lip **Rh** rhombencephalon **RN** red nucleus **rn** reticular neurons **so** somites **T** telencephalon **tb** tail bud **Th** thalamus **V** trigeminal ganglia **VIII** vestibular ganglia **Vn** trigeminal neurons **vn** vestibular neurons **zli** zona limitans intrathalamica

Instituto de Neurociencias de Alicante, CSIC-UMH. Campus de San Juan, Alicante, Spain
Grant sponsor: DIGESIC-MEC; Grant number: BFI2002/02979; Grant number: LSHG-CT-2004-512003; Grant number: BFU2005-09085; Grant number: BFU2005-23722-E/BFI and IP from EU LSHG-CT-2004-512003; Grant sponsor: Spanish MEC; Grant number: BFI2002/02979; Grant sponsor: Juan de la Cierva Program; Grant number: MEC2006.
[†]Dr. Gimeno's present address is Servicio de Inmunología. Hospital Universitario Virgen de la Arrixaca (HUVA), Ctra. Madrid-Cartagena s/n. 30120. Murcia, Spain.
[*]Correspondence to: Salvador Martinez, Instituto de Neurociencias UMH-CSIC, Universidad Miguel Hernandez, N-332, Km 87. E-03550 Alicante, Spain. E-mail: smartinez@umh.es

DOI 10.1002/dvdy.21237
Published online 24 July 2007 in Wiley InterScience (www.interscience.wiley.com).

they present mitogenic and angiogenic effects in cancer progression and active migratory effects in metastasis (reviewed in Goldfarb, 1996; Powers et al., 2000; Ornitz and Itoh, 2001). Fgfs interact with Fgf-tyrosine-kinase receptors (FgfR) to mediate the regulation of cell proliferation, migration, survival, differentiation, growth, and cell identity (Goldfarb, 1996; Ornitz et al., 1996; Powers et al., 2000). To date, at least 23 members of the family have been described (or 22 considering the orthology of *Fgf15* and *Fgf19*; Itoh and Ornitz, 2004) and are present in a wide range of animals, from nematodes to humans. Several *Fgf* genes are expressed during development in specific spatiotemporal patterns, suggesting a tightly regulated program of their functions in developmental processes. The overlap in their spatial and temporal expression patterns during development could suggest either a functional redundancy or a synergic action in their functions.

The roles of some Fgf proteins in development have been previously analyzed (for a review, see Powers et al., 2000). For example, it is well known that Fgf8 expression in the isthmus controls mesencephalic and rostral rhombencephalic development (including the cerebellum; Crossley and Martin, 1995; Crossley et al., 1996; Martinez et al., 1999; Joyner et al., 2000; Chi et al., 2003). This protein is also important for the patterning of the anterior neural plate (Shimamura and Rubenstein, 1997; Storm et al., 2006) as well as in limb development (Martin, 1998). Other Fgfs also play important functional roles. For instance, *Fgf3*, *Fgf8*, *Fgf10*, and, more recently, *Fgf19* have been shown to be important signals for the induction of inner ear development (Represa et al., 1991; Mahmood et al., 1995; Ladher et al., 2000, 2005; Leger and Brand, 2002; Maroon et al., 2002; Wright and Mansour, 2003; Sanchez-Calderon et al., 2006). Other factors, such as *Fgf2*, *Fgf4*, *Fgf8*, and *Fgf10* play a role in the establishment and initial development of the limb bud (Martin, 1998).

Previously, we published an exhaustive study of mouse *Fgf15* expression during neural tube development (Gimeno et al., 2002, 2003). Recently, an orthology between human and chick *Fgf19* and mouse and rat *Fgf15* genes has been suggested, based on molecular data (Nishimura et al., 1999). Both human *Fgf19* and mouse *Fgf15* contain three exons, as seen in the prototypical *Fgf* gene, with analogous distribution and size. Throughout the various studied species, the majority of the Fgf proteins are highly conserved and share greater than 90% amino acid sequence identity, with the exception of human *Fgf19* and mouse *Fgf15*, which only share approximately 50% (Katoh and Katoh, 2003; Wright et al., 2004). Some Fgfs are clustered within the genome; this is the case of the human *CCND1-Fgf19-Fgf4-Fgf3* cluster in chromosome 11q13 and the mouse *CCND1-Fgf15-Fgf4-Fgf3* cluster in chromosome 7(72.4) (Katoh, 2002; Katoh and Katoh, 2003). This evolutionary conservation supports the orthological correlation between both genes, despite their sequential difference (Katoh and Katoh, 2003). Other Fgf conserved clusters have been described (Ornitz and Itoh, 2001; Katoh, 2002), and in most cases, these clusters have been functionally related to carcinogenic processes (Katoh, 2002). From a developmental and functional perspective, both *Fgf19* and *Fgf15* have been related with otic embryonic induction (Graham, 2000; Ladher et al., 2000; Wright et al., 2004) and eye development (Kurose et al., 2004).

In this work, we study in detail the *Fgf19* expression pattern during chick neural tube development in comparison to the expression pattern of *Fgf15* in mouse. In addition, experimental data suggest that *Fgf19* expression in the isthmus is regulated by Fgf8, as seen in the development of the lens (Kurose et al., 2005). We also demonstrate, as original data, that *Fgf19* diencephalic–mesencephalic expression is regulated by *Shh* expressed in the zli and in the midbrain basal plate, as it has been seen in zebrafish *Fgf19* (Miyake et al., 2005) and the mouse ortholog *Fgf15* (see below and Ishibashi and McMahon, 2002).

RESULTS AND DISCUSSION

Comparative Analysis of Chick *Fgf19* and Mouse *Fgf15* Expression Patterns in the Neural Tube

The chick *Fgf19* expression pattern was analyzed by in situ hybridization (ISH) on whole-mount embryos at early stages of development (Hamburger and Hamilton stage [HH] 8–HH26). Embryonic brain sections (160 μm thick) were also processed by ISH and stained with neutral red to explore its expression at the cellular level, as well as in older developmental stages (HH17–HH41). Neural tube morphology and histogenetic maturation were meticulously considered to compare homologous stages and to establish adequate correlations between the *Fgf19* expression pattern in chick embryos and our reported data on *Fgf15* expression pattern in mouse embryos (Gimeno et al., 2003).

We first detected *Fgf19* mRNA in chick embryos at stage HH8 (four somites), when the neural tube was still open and the neural folds only met at the midbrain level. Whereas chick *Fgf19* was exclusively localized in the presumptive territory of the epibranchial placodes and in the mesoderm adjacent to the caudal hindbrain (Fig. 1A; Ladher et al., 2000, 2005; Wright et al., 2004), mouse *Fgf15* was expressed early in development at the neural plate stages in the anterior neural ridge and the rhombencephalon (Gimeno et al., 2003). In HH14 chick embryos, the *Fgf19* expression domain was maintained in the epibranchial placodes and mesoderm around the otic vesicle (Fig. 1B; Kurose et al., 2004; Sanchez-Calderon et al., 2006). A weak *Fgf19* expression was also observed both in the optic stalk and optic vesicle and was maintained until at least HH26 (Figs. 1, 3). From HH16 to HH30, *Fgf19* expression in the mantle zone of the isthmus appeared closely related to *Fgf8* ventricular expression (see Figs. 1C–I, 3A–C,Q–T). Mouse *Fgf15* was expressed in the anterior telencephalon, optic vesicle, thalamus, mesencephalic and anterior rhombencephalic alar plates, with a negative gap corresponding to the isthmic region, at stages E9.5–E11.5 (Fig. 1K; and Fig. 1 in Gimeno et al., 2003). Therefore, *Fgf19* expression in chick embryos (HH20) and *Fgf15* expression in mouse embryos (E9.5) presented complementary expressions in the isthmic mantle layer. This isthmic expression domain was also described by Kurose et al. (2004); however, we have precisely localized this expression in the

mantle layer of *Fgf8*-expressing neuroepithelium (Fig. 5A–C). This *Fgf8*-ventricular/*Fgf19*-mantle–positive traversal domain corresponded to the *Fgf15*-negative band in mouse (Fig. 5G).

Between HH19 and HH24, *Fgf19* expression was maintained in the dorsal half of the chick optic cup, as was seen in the mouse *Fgf15* (Fig. 1K), while the lens also showed a strong in situ reaction (Fig. 1D,E). From HH19 to HH26, a new longitudinal domain of *Fgf19* expression appeared in the mesencephalic and caudal diencephalic basal plate (Fig. 3A–C,E–G,I). This column of expression was localized rostral to the III nerve nucleus, in the mantle layer of the parabasal plate (Figs. 1E,I, 3A–C,E–G,I–J,U–V). Although Kurose et al. (2004) described this expression domain as ventral midbrain expression, it extended rostrally into the caudal diencephalon (pretectum) and was localized in a dorsal column of neuronal progenitors in the basal plate, which corresponds to the parabasal band described by E. Puelles in the basal plate (Puelles, 2000). In addition, we have detected a new basal domain localized caudally in the isthmus (Is) and rhombomere 1 (r1; Figs. 1I, 3A,B,E–G,I,N,R,T,V). Although Kurose et al. (2004) also identified the expression of *Fgf19* in the rhombic lip, its expression in the basal plate of the caudal rhombencephalon was not previously described. Here, a columnar pattern of *Fgf19*-expressing cells appeared repetitively distributed in consecutive rhombomeres, from r2 to r7, with differential expression levels, stronger in r3 and decreasing bilaterally in consecutive rhombomeres. The r4/r5 inter-rhombomeric boundary also presented stronger expression (Fig. 1F,H).

The trigeminal (V) and vestibular (VIII) ganglia, in the chick cephalic region, and the spinal ganglia expressed *Fgf19* from stages HH19 to HH24 (Figs. 1D–G, 3D; Kurose et al., 2004; Sanchez-Calderon et al., 2006). At these early developmental stages, positive reaction was also seen in the ventral epithelium of the four branchial pouches (Fig. 1D,E,G; Kurose et al., 2004), as well as in the tail bud (Fig. 1D,G) and the apical limb ectodermal ridge (AER; Fig. 1D,G).

Of particular interest, *Fgf19* was detected in the chick diencephalon from stages HH20 to HH26. This result was not reported previously. *Fgf19* mRNA was observed in the mantle layer of the alar plate, localized in a transversal strip corresponding to the zona limitans intrathalamica (zli, Figs. 1G, 3A,H,I,L,O,P). This expression was first detected at HH20, together with a strip of scattered positive cells connecting the diencephalon parabasal expression with the zli region (Figs. 1I, 6A–C). In the zli, *Fgf19* expression was maintained until stage HH26, localized in the mantle layer and radially related to the ventricular expression of *Shh* gene (Fig. 3O,P). As was seen in the isthmic region with *Fgf19*, the expression pattern in the zli was complementary to mouse *Fgf15* in the diencephalon. Whereas *Fgf15* was expressed in the mouse embryo on both sides of the zli but not directly in the zli (Fig. 1K), *Fgf19* was expressed in the mantle layer of chick zli (Fig. 1G,I,J). Between HH27 and HH38, *Fgf19* expression was only localized in scattered cells within several nuclei of the mesencephalon and rhombencephalon, mainly in pontine reticular neurons and in close relation to the nuclei of the vestibulocochlear system (Fig. 2A–J; Marin and Puelles, 1995; Sanchez-Calderon et al., 2006).

At stage HH38, a localized weak *Fgf19* expression was found for the first time in the cerebellum, specifically at the caudal end of the immature Purkinje cell layer (PCL; Fig. 2H′). At HH41, *Fgf19* was localized exclusively in the Purkinje cell layer of the two caudal folia (Fig. 2I,I′). In the rhombencephalon, *Fgf19*-expressing cells were distributed in a longitudinal column across different pseudorhombomeric domains, corresponding to the area of the hypoglossal nucleus (mXII; Cambronero and Puelles, 2000). This report is the first time that the expression of *Fgf19* has been described at late stages of development. Compared with mouse *Fgf15* expression in the perinatal period and at postnatal day 7, no similarities were noted with chick *Fgf19* expression (compare Figs. 3–5 in Gimeno et al., 2004, with Fig 2). However, some degree of complementary expression was present at the level of the PCL. Nevertheless, *Fgf15* was expressed mainly in anterior folia of mouse cerebellum, while *Fgf19* was localized in the two caudal most folia of the chick cerebellum (compare Fig. 2I with Fig. 4C in Gimeno et al., 2003).

Fgf19 in Relation to *Fgf8* and *Shh* Expression

Fgf19 expression was localized in differentiating neurons close to the morphogenetic centers identified as secondary organizers, the zona limitans intrathalamica (zli) in the diencephalon and the isthmic organizer (IsO) in the mid–hindbrain boundary (Echevarria et al., 2003; Martinez, 2001). This was also observed for mouse *Fgf15*, whose expression pattern was complementary to *Fgf19*, that is, while chick *Fgf19* was expressed in zli and isthmic mantle layers, *Fgf15* was expressed in mouse just outside of the zli and isthmic neuroepithelium (Figs. 1K, 5H–I, 6L; Gimeno et al., 2002, 2003).

At HH19, *Fgf19* transcripts were detected in the mantle at the level of the isthmic constriction (Figs. 1D–I, 3A–I,Q–T), where *Fgf8* was also expressed. This expression was maintained until at least stage HH30, confined to the mantle layer of the dorsal isthmic region adjacent to *Fgf8* ventricular expression (Fig. 3Q,S). A group of scattered cells in the basal plate of the isthmus and rhombomere 1 (r1) also strongly stained for *Fgf19*; these cells were localized close to the trochlear nucleus (IV; Figs. 1I, 3A,B,E–G,I,N,R,T). Positive cells in the isthmic basal plate were densely grouped and extended caudally to form a column into r1, where a decreasing cell concentration could be observed (Figs. 1I, 3A,B,E–G,I,N,R,T). Mouse *Fgf15* was expressed in the neuroepithelium at both sides of the isthmic constriction, rostrally in a rostrocaudal increasing gradient in the mesencephalic vesicle and, caudally in a caudorostral increasing gradient in r1, leaving an empty gap filled by Fgf8 expression (see Figs. 1K, 5H; Gimeno et al., 2002, 2003). In more anterior levels, *Fgf19* was expressed in a parabasal longitudinal domain at the mesencephalic–diencephalic limit (Fig. 1D,E,I, 3A–C,E–G,I,J,M,U–V). This expression was located within the mantle layer of the parabasal plate,

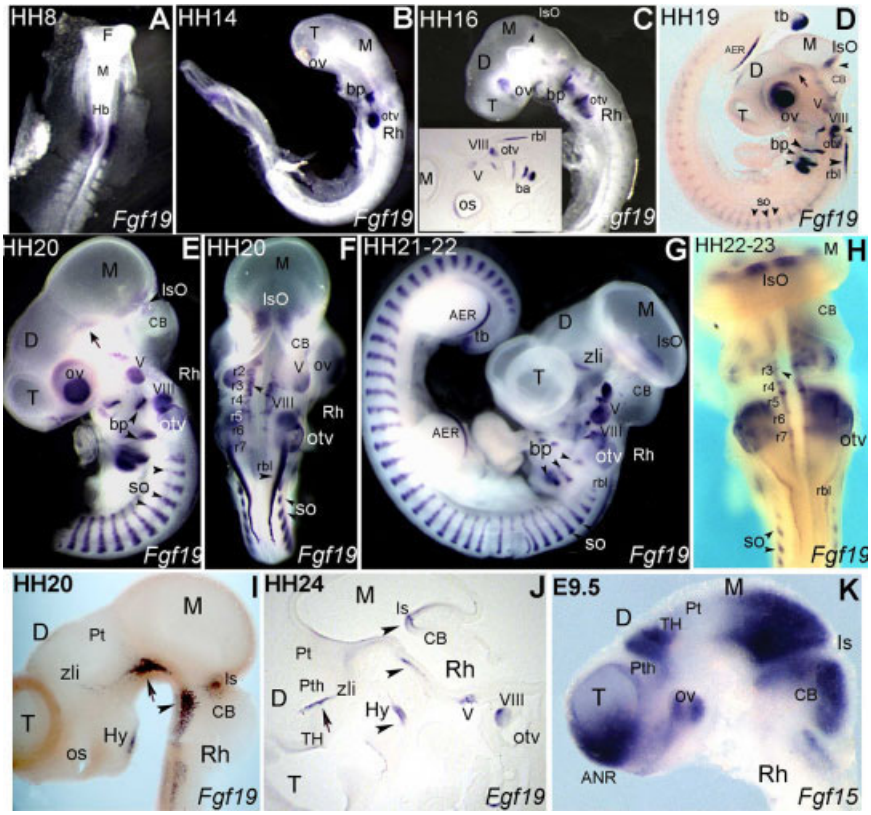

Fig. 1.

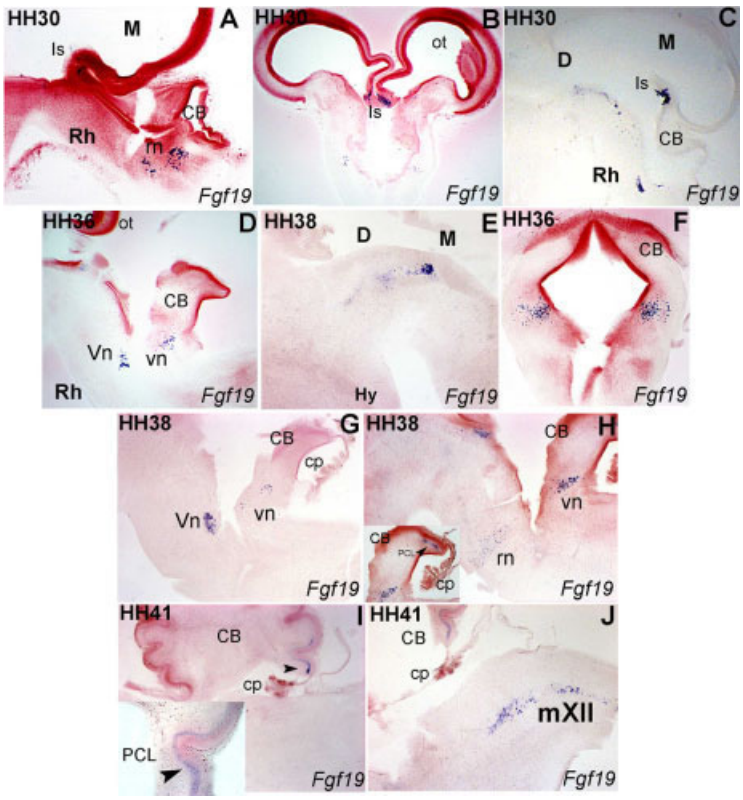

Fig. 2.

which was characterized by *Shh* expression in the radially related neuroepithelium (Fig. 3E–G,I–J,M). However, because *Shh* was exclusively expressed in the neuroepithelial cells and *Fgf19* was only expressed in mantle layer, there was no coexpression of *Shh* and *Fgf19* (Fig. 3J and M). These *Fgf19*-positive cells were localized dorsal and rostral to III nerve nucleus, identified by Islet1 expression (Fig. 3U,V). By their localization, they might correspond to the red nucleus and/or the interstitial reticular nucleus in the midbrain and pretectal basal plates (Garcia-Lopez et al., 2004). *Fgf19* and *Shh* did not coexpress in the diencephalic zli, as observed in horizontal sections of HH22 chick embryos (Fig. 3L,O,P), as a result of the differential localization in the radial dimension of the neural wall. In mouse, *Fgf15* and

Fig. 1. A–K: *Fgf19* expression pattern at early stages of chick development compared with mouse *Fgf15* expression. A–D: *Fgf19* transcripts were detected in the presumptive territory of the epibranchial placodes and mesoderm adjacent to the otic vesicle, at Hamburger and Hamilton stage (HH) 8 (otv; A,B), and at the optic vesicle from HH19 to HH22 (ov; B–D). D–H,J: From HH19 to HH23, *Fgf19* expression was also detected in the tail bud (tb), apical ectodermal ridge (AER), somites (so), branchial pouches (bp), isthmic constriction (IsO), V and VIII ganglia (V and VIII), as well as in the rhombic lip (rbl; arrowheads). In the neural tube, *Fgf19*-positive cells were localized in the rostral mesencephalic and caudal diencephalic basal plates (D,E,I, arrows) as well as in the r1 basal plate (I, arrowhead). Arrowheads in J label *Fgf19* expression in the isthmic (Is), rhombomere 1 (Rh), and caudal hypothalamic (Hy) regions. I,J: From HH20 to HH24, *Fgf19* was localized in the zona limitans intrathalamica (zli). K: *Fgf15* presented a complementary expression pattern in the secondary organizers, IsO and zli organizers, but different to *Fgf19* expression.

Fig. 2. Expression of chick *Fgf19* at later developmental stages. **A–C:** At Hamburger and Hamilton stage (HH) 30, *Fgf19* was still expressed in the isthmic region (Is). **D–G:** From HH36 to HH38, *Fgf19* was detected in the mesencephalic tegmentum as well as in several rhombencephalic nuclei: pontic reticular neurons, which form part of the nuclei of the vestibular-cochlear system (vn; D–F), and the trigeminal nucleus (Vm; G). **H–J:** Between HH38 and HH41, *Fgf19*-scattered positive cells appeared in the caudal end of the Purkinje cell layer (PCL; arrowheads). At HH41, *Fgf19*-expressing cells were also localized in the area of the hypoglossal nucleus (XIIm).

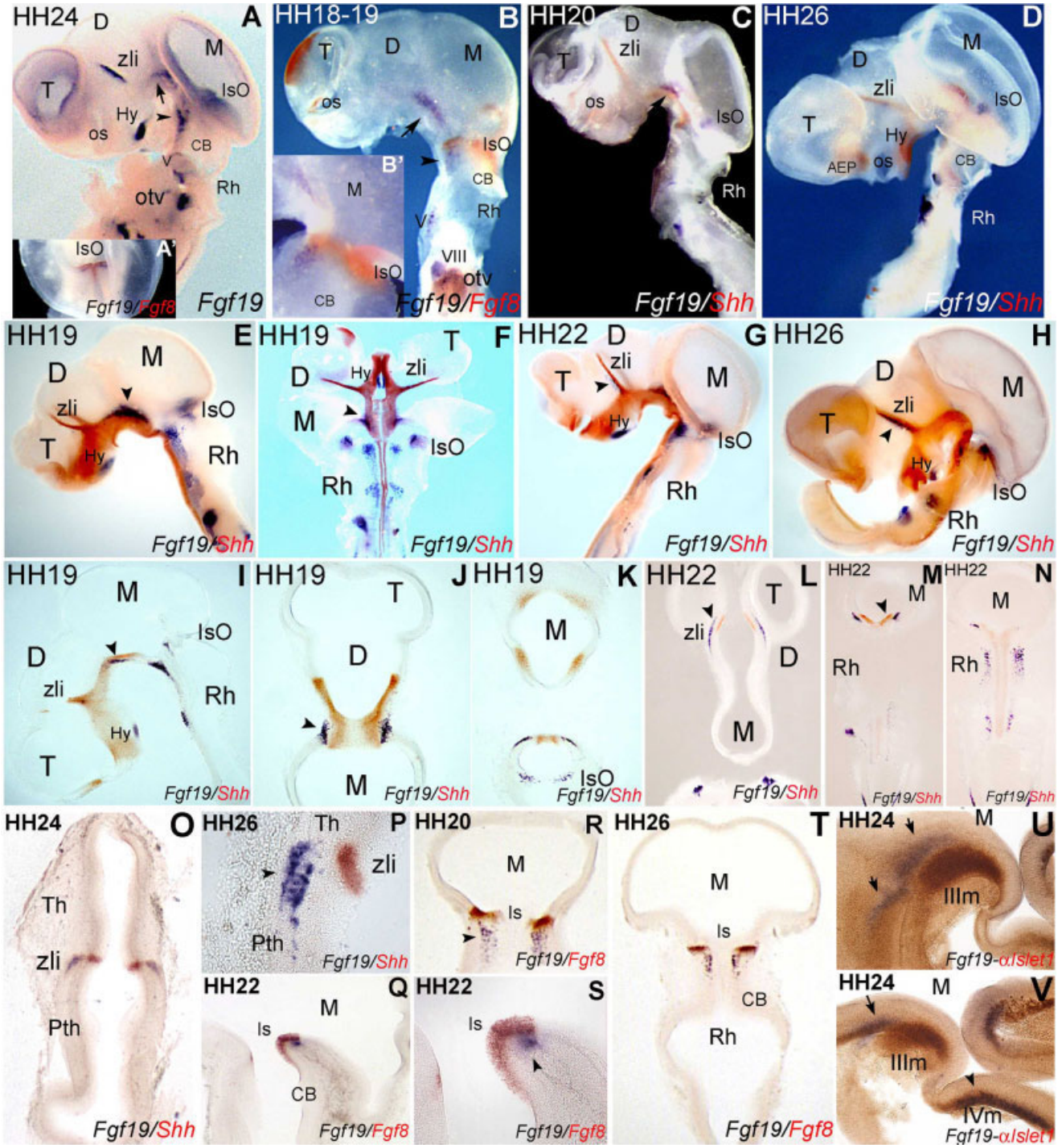

Fig. 3. **A–V:** *Fgf19*, *Fgf8*, and *Shh* expression patterns in the chick neural tube. *Fgf19* and *Fgf8* were colocalized in the alar plate of the isthmus (A–H,Q–T). *Fgf19* was localized in the mantle layer, in close relation to *Fgf8* neuroepithelial expression (Q–T, arrowheads). A group of scattered cells in the isthmic basal plate and rhombomere 1 presented strong *Fgf19* expression and were detected close to the trochlear nucleus (IVm; A,E–G,I,N,R,T, and V; arrowheads in A,B and D; arrow in U,V). *Fgf19* basal expression was colocalized with *Shh* (E–N) in the mesencephalic and diencephalic basal plates (E–G,I [arrows],J,M [arrowhead]). This expression corresponded to a lateral column inside the *Shh* band in the neuroepithelium (E–G,I,J,M), localized rostral to the III nerve nucleus that was identified by Islet 1 expression (U,V). *Fgf19* expression in the zli presented a radial correlation to *Shh* ventricular expression in this region (L,O,P, arrowhead).

Shh did not overlap spatially, due to their respective exclusive domains in the neuroepithelium. This suggests that, in chick, the possible regulation of *Fgf19* by Shh signaling may occur in clonally related cells (cell autonomous mechanisms), whereas in mouse the suggested relation of *Fgf15* expression and Shh (Ishibashi and MacMahon, 2002; Saitsu et al., 2005) may be a consequence of signaling mechanisms (not cell autono-

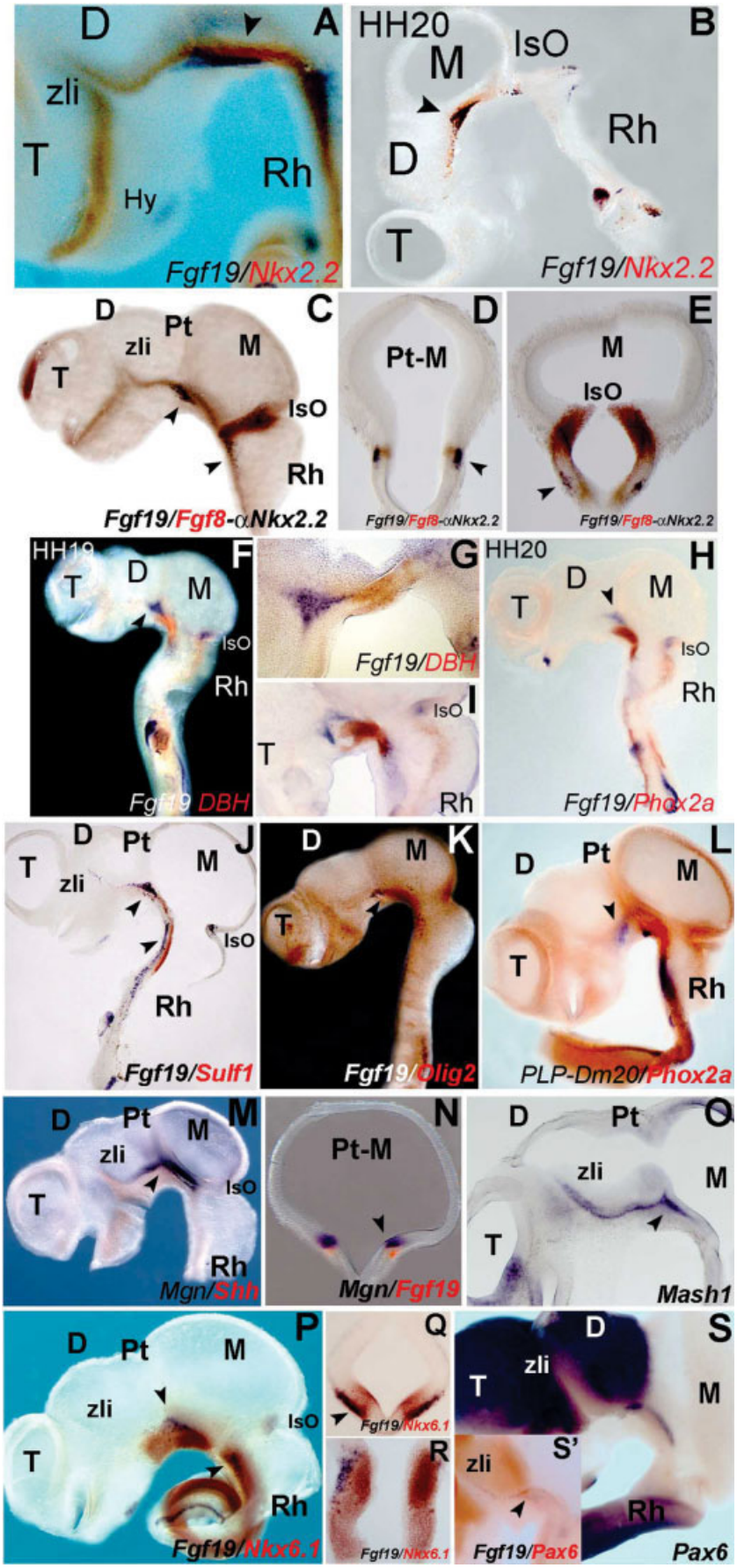
A
D
zli
T
Hy
Rh
Fgf19/Nkx2.2
B
HH20
M
lsO
D
Rh
T
Fgf19/Nkx2.2
C
D
Pt
zli
M
T
lsO
Rh
Fgf19/Fgf8-αNkx2.2
D
Pt-M
Fgf19/Fgf8-αNkx2.2
E
M
lsO
Fgf19/Fgf8-αNkx2.2
F
T
D
M
lsO
Rh
Fgf19/DBH
G
Fgf19/DBH
I
lsO
T
Rh
HH20
H
D
M
T
lsO
Rh
Fgf19/Phox2a
J
D
Pt
M
T
zli
lsO
Rh
Fgf19/Sulf1
K
D
M
T
Fgf19/Olig2
L
D
Pt
M
T
Rh
PLP-Dm20/Phox2a
M
D
Pt
M
zli
T
lsO
Rh
Mgn/Shh
N
Pt-M
Mgn/Fgf19
O
D
Pt
zli
M
T
Mash1
P
D
Pt
M
zli
T
lsO
Rh
Fgf19/Nkx6.1
Q
Fgf19/Nkx6.1
R
Fgf19/Nkx6.1
S
D
zli
T
M
S'
zli
Rh
Fgf19/Pax6
Pax6

Fig. 4.

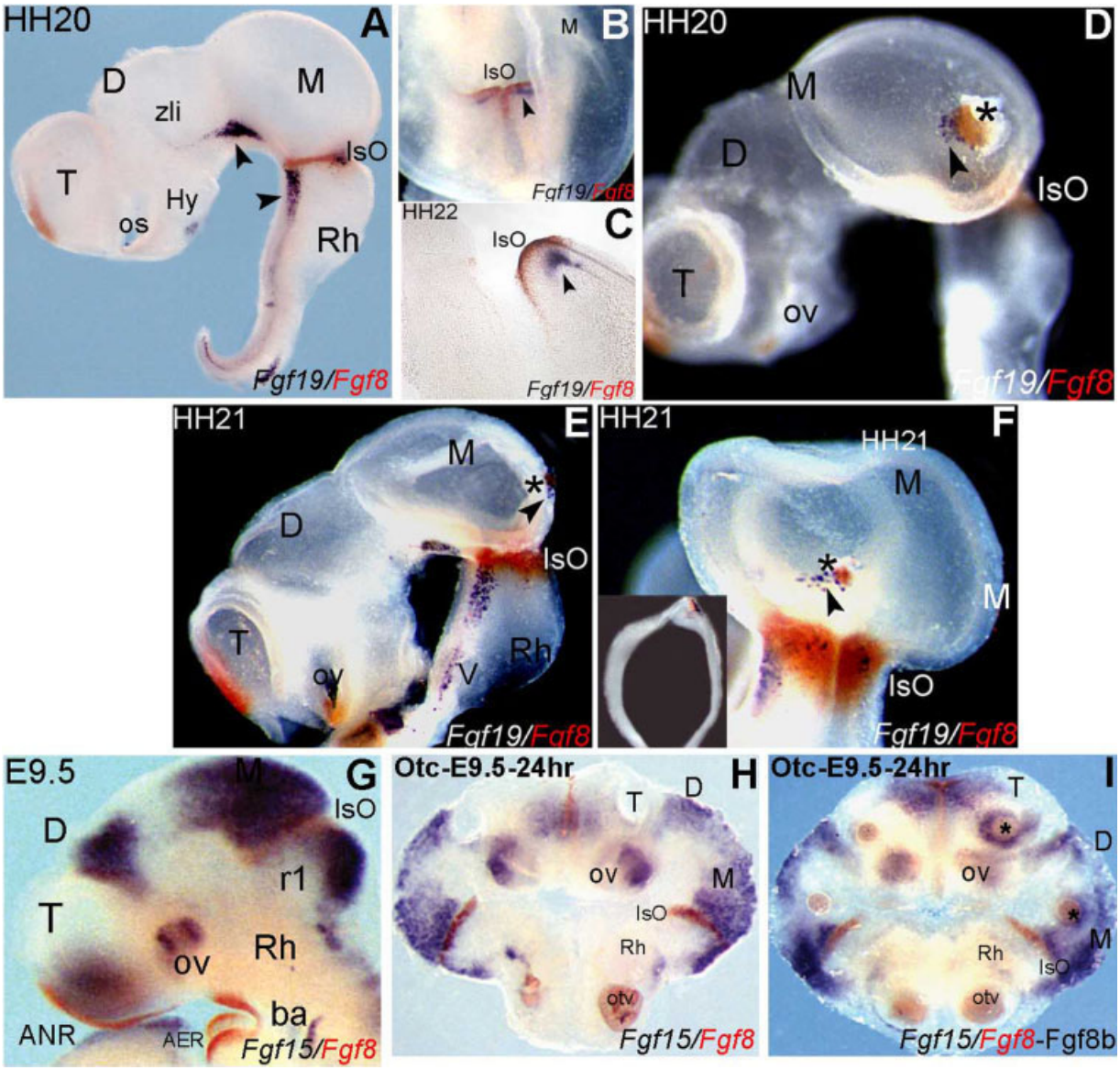

Fig. 5. *Fgf19* and *Fgf15* expression was ectopically induced by Fgf8 protein. **A–C:** *Fgf19* and *Fgf8* colocalized in the isthmic alar plate. Whereas *Fgf19* was detected in the mantle layer (arrowhead in B,C), *Fgf8* localized in the ventricular epithelium (B,C). **D–F:** The insertion of Fgf8-soaked beads (asterisk) in the alar plate of the caudal mesencephalic vesicle led to the ectopic expression of *Fgf19* in scattered cells around the bead (arrowheads). **G:** *Fgf15* (blue) expression was localized around the isthmic organizer, in a decreasing gradient of expression from the isthmus, as well as in the caudal mesencephalon and in rhombomere 1 (r1), in a complementary pattern with *Fgf8* (red) isthmic expression. **H,I:** *Fgf15-Fgf8* expression was maintained for 24 hr in mouse explant cultures (H) and *Fgf15* expression was ectopically induced by Fgf8-soaked beads in rostral prosencephalon and mesencephalon (asterisk in I).

Fig. 4. Molecular phenotype of *Fgf19*-expressing cells. *Fgf19*-expressing cells were analyzed in relation to the expression of other genes. **A–E:** *Nkx2.2* gene (A,B, arrowheads) and protein expression patterns (C–E, arrowheads). *Nkx2.2* was expressed in the epithelium, while *Fgf19* transcripts were localized superficially in the mantle layer. **F–H:** *DBH* and *Phox2a* were expressed in near but different domains than *Fgf19* (arrowheads). **J–L:** *Fgf19* were coexpressed with *Sulf1*, *Olig2*, and *PLP-Dm20*. **M–O:** *Fgf19* was coexpressed with *Mgn* and localized in *Mash1*+ domain (arrowheads). **P–S′:** *Nkx6.1* and *Pax6* expression patterns were also colocalized with the *Fgf19*-expressing band in the mantle layer (arrowheads).

mous) occurring between neuroepithelial cells.

Fgf19 Is Expressed in Molecularly Heterogeneous Neuroepithelial Cells

To determine the phenotype of *Fgf19*-positive cells in the parabasal columns at the midbrain–forebrain boundary and at r1, we analyzed the expression of other developmental genes that mapped into or close to these domains. To this end, we examined *Nkx2.2* expression in conjunction with *Fgf19*. From a lateral view of the neural tube (HH20), mesencephalic *Fgf19* expression was localized at the level of the *Nkx2.2*-positive band (Fig. 4A–C). *Fgf19*-expressing cells were also detected in the mantle layer, peripheral to *Nkx2.2* in the ventricular layer (Fig. 4D,E).

The expression of *Fgf19* was also analyzed together with other neural cell specific markers, such as *DBH* and *Phox2a* (catecholaminergic cell markers) (Fig. 4F–H); *Sulf1*, *Olig2*, and *PLP-Dm20* (markers of oligodendrocyte pre-

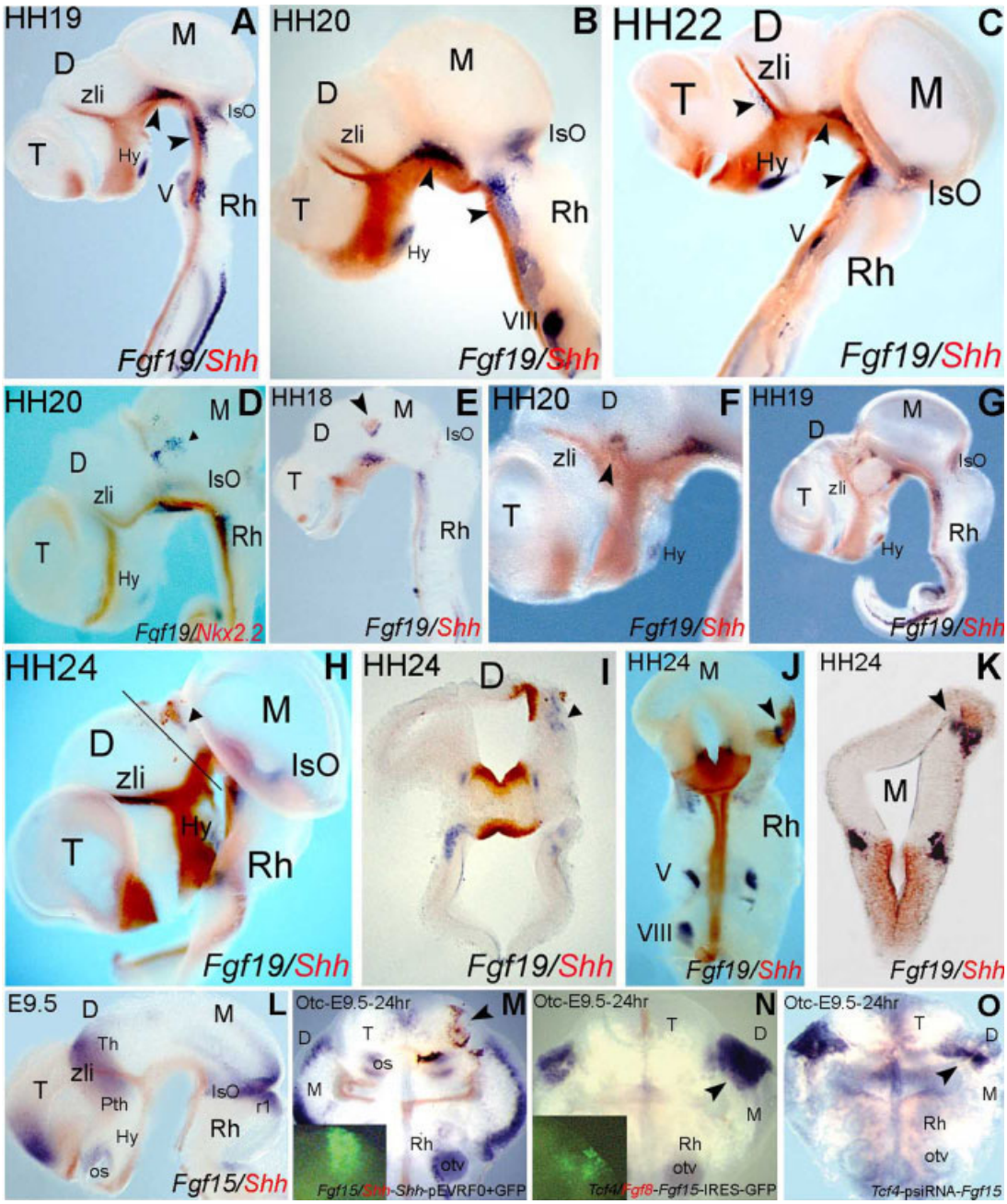
HH19
A
M
D
zli
IsO
T
Hy
V
Rh
Fgf19/Shh
HH20
B
M
D
zli
IsO
T
Rh
Hy
VIII
Fgf19/Shh
HH22
D
C
zli
T
M
Hy
IsO
V
Rh
Fgf19/Shh
HH20
M
D
D
zli
IsO
T
Rh
Hy
Fgf19/Nkx2.2
HH18
E
M
D
IsO
T
Rh
Fgf19/Shh
HH20
D
F
zli
T
Hy
Fgf19/Shh
HH19
M
G
D
IsO
T
zli
Rh
Hy
Fgf19/Shh
HH24
H
M
D
IsO
zli
Hy
T
Rh
Fgf19/Shh
HH24
D
I
Fgf19/Shh
HH24
M
J
Rh
V
VIII
Fgf19/Shh
HH24
K
M
Fgf19/Shh
E9.5
D
M
L
Th
zli
T
Pth
IsO
r1
Hy
Rh
os
Fgf15/Shh
Otc-E9.5-24hr
M
D
T
os
M
Rh
otv
Fgf15/Shh-Shh-pEVRF0+GFP
Otc-E9.5-24hr
N
T
D
M
Rh
otv
Tcf4/Fgf8-Fgf15-IRES-GFP
Otc-E9.5-24hr
O
T
D
M
Rh
otv
Tcf4-psiRNA-Fgf15

Fig. 6.

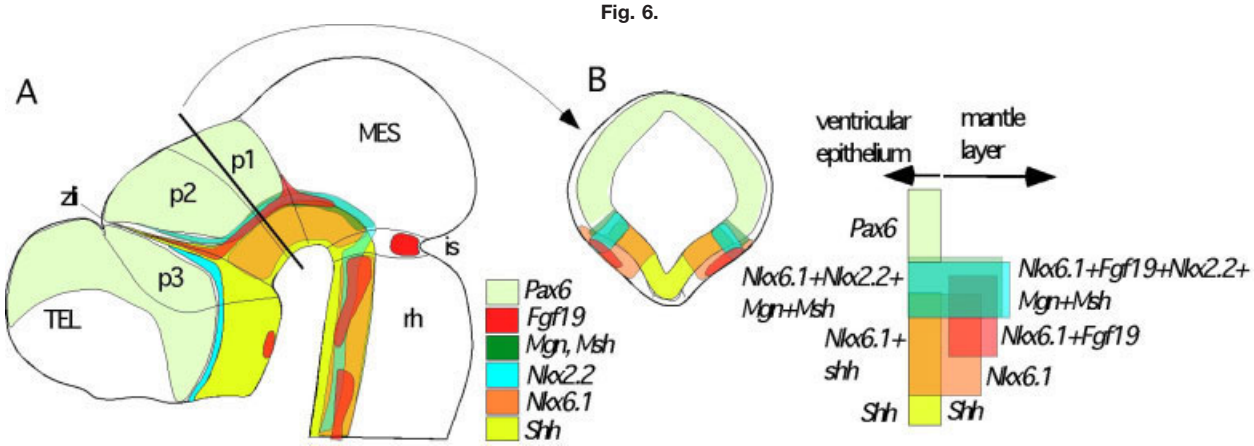
A
B
MES
p1
p2
zli
p3
TEL
is
rh
Pax6
Fgf19
Mgn, Msh
Nkx2.2
Nkx6.1
Shh
ventricular epithelium
mantle layer
Pax6
Nkx6.1+Nkx2.2+ Mgn+Msh
Nkx6.1+Fgf19+Nkx2.2+ Mgn+Msh
Nkx6.1+ shh
Nkx6.1+Fgf19
Nkx6.1
Shh
Shh

Fig. 7.

cursors; Fig. 4J–L); and finally with *Mgn* and *Mash1*, as γ-aminobutyric acid GABAergic progenitor markers (Fig. 4M–O). Moreover, we also mapped the *Nkx6.1* and *Pax6* expression patterns to compare with *Fgf19* localization in the basal plate (Fig. 4P–S). The analysis of these combined experiments confirmed the interpretation of *Fgf19*-expressing cells as forming a cellular column of the parabasal plate, which corresponds to a ventricular domain expressing *Shh*, *Nkx2.2*, *Nkx6.1*, *Mash*, and *Mgn*. In the mantle layer, cells coexpressed *Nkx6.1*, *Sulf-1*, *Mgn*, and *Pax6*, in addition to *Fgf19*.

Therefore, *Fgf19* expression was transiently detected in a cellular band of the parabasal plate in the mantle layer of the caudal diencephalon (prosomeres 1 and 2) as well as in the rostral mesencephalon, between embryonic stages HH19 and 26. This longitudinal domain corresponds to a dorsal column in the prospective prerubral and pretectal tegmentum that were traversed by the medial longitudinal fascicle (mlf; Easter et al., 1993; Garcia-Lopez et al., 2004), which was named the parabasal band by Puelles (Puelles, 2000). This parabasal region seems further characterized by the expression of *Pax6*, *Mgn*, *Mash*, *Sulf1*, *Olig2*, and *PLP-Dm20* in the neuroepithelium (Figs. 4, 7), as well as by acetylcholinesterase histochemistry and by the expression of other homeobox genes (Sanders et al., 2002; Schubert and Lumsden, 2005). Some of these *Fgf19*-expressing cells coexpress *Nkx6.1*, which has been proposed as a marker of red nucleus cells (Barth and Wilson, 1995; Puelles et al., 2004). In addition, *Fgf19*-positive cells establish close topographical relations with the expression domains of genes transcribed in GABAergic neurons (Guillemot and Joyner, 1993; Guimera et al., 2006) and oligodendrocytes (Perez-Villegas et al., 1999; Thomas et al., 2000). Our double-staining experiments resulted in a coexpression of *Fgf19* with several GABAergic and oligodendroglial markers: *Mgn* and *Olig2*, *PLP/dm20*, and *Sulf1*, respectively. This finding is in agreement with a recent report where, in the zebrafish forebrain, the induction of *Fgf19* expression is related to GABAergic and oligodendroglial differentiation (Miyake et al., 2005). It is possible that the transient *Fgf19* expression may be involved in cell fate regulation; however, to prove this involvement, it would be necessary to perform experiments of gain and loss of function.

Later in development, the mantle area displaying *Fgf19*-positive cells extended rostrally, from p1 through the parabasal mantle layer of p2, to the anterior limit of p2 and the zli. These *Fgf19* p2-expressing cells mapped the presumptive areas of the perirotundic area and interstitial nucleus of the optic tract, in the alar plate, and the rostral interstitial reticular nucleus of the pre-rubral tegmentum in the basal plate (Fig. 7). The presence of migrating oligodendroglial progenitors and GABAergic cells in this domain has been suggested, as seen by its coexpression with other molecular markers; however, we have not been able to localize *Fgf19* expression in cells that dispersed tangentially from this parabasal column. This does not eliminate the possibility that a tangential cellular migration occurred, and *Fgf19* expression was down-regulated once the migration of these cells commenced. In quail–chick transplant experiments, we have detected an important source of tangentially migrating cells coming from these parabasal regions (S. Martinez and R. Garcia-Lopez, personal observation).

FGF8 Protein Induces Ectopic Expression of *Fgf19*

The expression of *Fgf19* was closely related to *Fgf8* in the isthmic organizer (IsO; Martinez, 2001; Fig. 5A–C). Whereas *Fgf8* expression corresponded to a transversal neuroepithelial domain in the isthmic constriction, *Fgf19* was expressed in a narrow zone of the local alar mantle layer, radially related to the expression of *Fgf8* in the neuroepithelium (Fig. 5A,D,E).

We have observed that Fgf8-soaked beads implanted in mesencephalon or prosencephalon of E9.5 mouse explants ectopically induced *Fgf15* expression in the neuroepithelium surrounding the Fgf8 beads (Fig. 5H,I; no effect was seen by inserting phosphate buffered saline [PBS] -soaked beads). These results are in agreement to the Fgf8-*Fgf15*-positive regulation reported in cardiac development (Saitsu et al., 2006). To determine whether Fgf8 regulates *Fgf19* expression in chick embryos, we implanted Fgf8-soaked microbeads in the midbrain alar plate in ovo. At 22 to 24 hr after the insertion, ectopic expression of *Fgf19* was detected in the cells surrounding the bead (Fig. 5D–F). Consequently, the observed effect could assign a positive role to Fgf8 in the regulation of *Fgf19* in the isthmus. In conclusion, our experimental data show that *Fgf19* in the chick isthmus and *Fgf15* in the mouse mesencephalon have similar functions in complementary patterns, and these orthologs are positively regulated by Fgf8 in both species. Therefore, it seems that, although the expression pattern evidences significant evolutionary variation, the Fgf8-dependent molecular regulatory mechanisms may have

Fig. 6. Shh regulates *Fgf19* and *Fgf15* expression in the rostral mesencephalon and caudal diencephalon. **A–C:** *Fgf19* was expressed in correlation with *Shh* in the basal plate of the rostral mesencephalon and caudal diencephalons (arrowheads). **D–K:** An ectopic source of Shh (*Shh* QT6-expressing cells) induced *Fgf19* expression (arrowheads) 24 hr after the cell insertion (E). E–K: This induction was observed caudal to the zona limitans intrathalamica (zli), in both the thalamus (F) and pretectum (D,E,G–I), as well as in the rostral mesencephalic vesicle (J,K). **L:** *Fgf15* presented a complementary pattern of expression with Shh in the zli of mouse embryos. **M:** The overexpression of *Shh* by microelectroporation induced *Fgf15* expression in the caudal telencephalon and diencephalon (arrowhead). **N,O:** Fgf15 mediated Shh signalling through the regulation of *Tcf4*, upregulated by *Fg15* overexpression (N, arrowhead), and down-regulated by psiRNA-Fgf15 (O, arrowhead).

Fig. 7. Schematic diagram that summarizes the *Fgf19* expression pattern in the developing chick neural tube in relation to other developmental genes. **A:** Representation of a neural tube lateral view. **B:** Diagram of a transverse section through the diencephalon at the level indicated by a black line. A: *Fgf19* expression (red) at the rostral mesencephalic–caudal diencephalic basal plates was localized in correlation to the neuroepithelial *Shh* (yellow) and *Nkx2.2* (blue) band, but restricted to the mantle layer (B). Other developmental markers were mapped in this territory: the γ-aminobutyric acid (GABA)ergic markers *Mgn* and *Mash* (green band), as well as *Nkx6.1* (orange band). *Fgf19* was coexpressed with *Nkx6.1* in this area. Fgf19 was also detected in the basal plate of r1, where *Nkx6.1* also coexpressed. Other *Fgf19*-positive domains discovered were the isthmic alar plate and a restricted expression in the basal plate of the hypothalamus.

been conserved. In cellular terms, the observed characteristic expression patterns of *Fgf19* and *Fgf15* in these two species can be explained by a difference in timing of the molecular specification of neuroepithelium, leading to a differential response of neuroepithelial cells to Fgf8 signaling in these two vertebrates. For instance, *Mkp3* gene expression in the mid–hindbrain region is heterochronically regulated in mouse and chick embryos by *Fgf8* expression in the isthmus. In mice, *Mkp3* is activated in the isthmic regions as soon as *Fgf8* is expressed (embryonic day 8.5; Echevarria et al., 2005a,b), whereas in chick embryos, it is activated 24 hr later: *Fgf8* appears at stage HH8–HH9 and *Mkp3* at stage HH13 (Vieira and Martinez, 2005). Although both chick *Fgf19* and mouse *Fgf15* were, respectively, activated in the isthmus or mid–hindbrain region, 24 hr after activation of *Fgf8* in the isthmus at stages HH16 in chick and E9 in mouse, HH16 chick embryos seem to be morphologically more mature than E9 mouse embryos and subsequently the receptive areas may show different potentialities. This difference in the signaling could be related to a differential pattern of morphogenetic induction due to a chronologically regulated modification of gap junction permeability in neuroepithelial cells (Martinez et al., 1992).

Shh QT6-Expressing Cells Induce Ectopic Expression of *Fgf19*

Fgf19-positive domains at the midbrain and caudal forebrain parabasal plates were localized in the mantle layer, corresponding to the dorsalmost area of neuroepithelial *Shh* expression (Fig. 6A–C). This finding suggests a possible regulation of *Fgf19* expression by Shh. To assess this point, we implanted *Shh*-QT6–expressing cells in ectopic domains of midbrain and diencephalon in ovo. Subsequently, ectopic expression of *Fgf19* was localized in the host mantle layer close to the grafted cells, both in the diencephalon caudal to the zli (Fig. 6F–I) and in the rostral mesencephalic vesicle (Fig. 6E,J,K), 24 hr after cell insertion.

Fgf19 transcripts in the chick mesencephalon and caudal prosomeres (p1–2) were localized in the mantle layer of the parabasal plate. This expression extends from the parabasal p2 domain to the cells of the mantle layer in the zli. All these *Fgf19*-expressing domains were related radially with *Shh* ventricular expression (Fig. 7).

We observed that *Shh*-expressing QT6 cells induced *Fgf19* expression when inserted in ectopic territories. It has been reported that Shh regulates the longitudinal molecular domains in the mesencephalic basal plate, a process that may be associated with the specification of cell fate properties in different neuroepithelial territories (Watanabe and Nakamura, 2000; Agarwala et al., 2001; Agarwala and Ragsdale, 2002). This longitudinal pattern in the mesencephalon could represent the continuation of the well-known longitudinal microzonal pattern described in the rhombencephalon and spinal cord (Ericson et al., 1995; Yamada et al., 1991). Therefore, the restricted columnar expression of *Fgf19* in mesencephalic and diencephalic neuroepithelium also may be related to the specification of cell fate domains. This columnar organization in the basal mesencephalon was interpreted as an "arcuate plan" by Sanders et al. (2002), referring apparently to the curves caused by the cephalic flexure in the flat-mounts, which can be misinterpreted as a radial pattern instead of the true longitudinal topological organization.

It is well known that Shh signaling plays an important role in the establishment of the ventrodorsal patterning in the ventral midbrain, in coordination with the control of its size (Agarwala et al., 2001). *Fgf19* expression in the parabasal mantle layer may represent a transient longitudinal domain where cells are induced to express this gene by a given concentration of Shh, and then committed to differentiate as neurons of the red nucleus and interstitial reticular nucleus of the mesencephalic and p1 tegmentum. Studies in zebrafish (Barth and Wilson, 1995; Miyake et al., 2005) and the combined expression of *Mgn* gene in this parabasal area in chicks (present results) suggest that the *Fgf19*-expressing cells could be specified to become both GABAergic neurons and oligodendrocyte progenitors in the mesencephalic basal plate. However, new experiments modifying *Shh* expression are necessary to characterize the direct correlation between Shh concentration and *Fgf19* expression in the parabasal diencephalon and mesencephalon, as well as its importance in cell fate specification.

Fgf19 expression in the mantle layer of zli can also be regulated by *Shh* in the zli neuroepithelium. In mouse, *Fgf15* was regulated by Shh; however, it was more broadly expressed in the neuroepithelium of the thalamus and prethalamus than *Fgf19* in the chick (Gimeno et al., 2002, 2003). In *Shh* knockout mice, an important reduction of the diencephalon was deduced from the lack of *Fgf15* expression (Ishibashi and McMahon, 2002). Despite the obvious differences in the expression patterns between chick *Fgf19* and mouse *Fgf15*, we concluded that *Fgf19* basal plate expression were regulated by *Shh*, as was demonstrated by *Fgf15* expression in mice (Ishibashi et al., 2005; Saitsu et al., 2005, present data; Fig. 6L–O). Regarding the restricted expression of *Fgf19* in the diencephalic alar plate, in relation to the extended expression of *Fgf15* in the mouse, a weaker phenotype can be predicted after Shh reduction in chicks and humans than in mice, as it was suggested by chick experiments (Vieira and Martinez, 2006), as well as by the absence of important thalamic anomalies in human holoprosencephaly caused by *Shh* mutations (Roessler et al., 1996, Schell-Apacik et al., 2003).

EXPERIMENTAL PROCEDURES

Cloning Chick *Fgf19*

The sequence of chick *Fgf19* gene was amplified using reverse transcriptase-polymerase chain reaction from HH8–HH26 mRNA chick embryos. The primers used were 5′-GTGCCCAGTTGCCATATTCG-3′ as forward primer and 5′-CTGACCTAGCACTTCATTGCC-3′ as reverse primer. The 1,084-bp amplified product was subcloned into pCR^{R}II- TOPO^{R} vector (Invitrogen) and was used as an ISH probe.

Chick Embryos

Chick embryos were obtained from fertilized eggs incubated at 38°C in a forced air incubator up to the desired embryonic stage. Chick embryos were staged according to the tables of Hamburger and Hamilton (1951) and the Atlas of Chick Development (Bellairs and Osmond, 1998).

Mouse Embryos and Organotypic Cultures

Mouse embryos were obtained by mating ICR mice. Embryos were isolated on the indicated stage after detecting the vaginal plug, considered 0.5 days post coitum in the timing of embryos. Mouse embryos were staged using morphological criteria (Kaufman, 1999). For organotypic cultures (explants), mouse E9.5 neural tubes were dissected and opened through the dorsal midline in Krebs medium. The explants were cultured as an open book in a 5% CO_2 incubator at 37°C for 24 hr, according to the technique described by Echevarria et al. (2001).

Fgf8 Protein Bead Implantation on In Ovo Chick and Mouse Explants

Heparin acrylic beads (Sigma) were soaked in a 0.1 M PBS solution containing 1 mg/ml of bFGF8 protein (R&D system, Minneapolis). After 1 hr of incubation at 4°C and several washes in PBS, the Fgf8 beads were inserted at different levels of the chick/mouse neural tube; experimental procedures were previously described (Crossley et al., 1996; Martinez et al., 1999; Garda et al., 2001).

In Ovo Implantation of SHH-Expressing QT6 Cells

Spherical cell aggregates of QT6-control and SHH-expressing QT6 cells were prepared as described by Duprez et al. (1996). Cell aggregates were implanted into the right side of the neural tube, after carefully opening the neuroepithelium, at different positions in HH10–HH11 chicken embryos and were left to develop until HH23–HH26. Afterward, the embryos were fixed overnight with 4% paraformaldehyde (PFA) in 0.1 M PBS at 4°C.

Mouse Explant Microelectroporation

Shh (cloned in pEVRF vector) plus GFP (cloned in pCAGGS vector) and *Fgf15* (cloned in IRES-GFP) expression vectors, along with the *Fgf15* RNAi vector (using the *Fgf15* sequence GAGGTGTCATGGCGAGAAAGT for psiRNA vector construction in ph7SKGFPzeo vector, Invivogene), were microelectroporated into mice E9.5 neural explants at different levels of the neural epithelium. A solution containing 1 μg/μl of the plasmid with Fast green (Sigma; 1:1,000) in 0.1 M PBS were loaded into micropipettes and injected into the neuroepithelium with a 5 volt, 50-msec rectangular pulse charge, according to the protocol described by Echevarria et al. (2005a).

Whole-Mount and Sectional In Situ Hybridization

ISH was performed on mouse and chick whole-mount embryos as well as in mice and chick brain sections. The brain samples were placed in agarose, and by using a Vibratome, 150-μm slices were obtained. Embryos were collected at different stages and fixed in 4% PFA at 4°C. The method for ISH was essentially as previously described by Shimamura et al. (1994). Digoxigenin and fluorescein RNA antisense probes for chick *Fgf19*, *Fgf8*, *Shh*, *Nkx2.2*, *DBH*, *Phox2a*, *Olig2*, *Sulf1*, *PLP-Dm20*, *Mgn*, *Mash*, *Nkx6.1*, and *Pax6* genes were prepared according to the instructions of the manufacturer (Roche).

Immunohistochemistry

After chick whole-mount ISH, immunostaining with islet-1 and Nkx2.2 monoclonal antibodies (1:10 and 1:20, respectively; Developmental Studies Hybridoma Bank, University of Iowa) were performed. After several washes in 0.1 M PBS containing 0.1% Triton X-100, the whole-mount embryos were blocked by incubation in 0.1 M PBS-0.1% Triton X-100-0.1 M Lysine for 1 hr and incubated with the anti–islet-1 or anti-Nkx2.2 overnight at 4°C. Subsequently, after several washes in PBS-0.1% Triton, mouse explants were incubated with a biotinylated goat anti-mouse IgG secondary antibody (1:300 in a PBS-0.1% Triton solution; Vector Laboratories) for 1 hr, rinsed in PBS-0.1% Triton and incubated for 1 hr in peroxidase-conjugated streptavidin (1:500, ABC Elite Kit, Vector Laboratories) in PBS. The staining reaction was performed with 0.05% 3,3′-diaminobenzidine and 0.01% hydrogen peroxide in 50 mM Tris-HCl pH 7.6. The embryos were embedded in agarose, and 75-μm sections were obtained using a Vibratome.

ACKNOWLEDGMENTS

This work was supported by Spanish Grants DIGESIC-MEC and IP from EU LSHG-CT-2004-512003. L. Gimeno was funded by the Spanish MEC and now is supported by the Juan de la Cierva Program and FFIS (CARM). We thank J. Guimera and W. Wurst for the helpful cloning of the *Fgf19* gene. We also thank J. Galceran for providing the Shh-pEVRF0 expression vector as well as J. Rubenstein (Shh, Nkx2.2, Nkx6.1, and Pax6), G. Martin (Fgf8), W.D. Richardson (Olig2), J. Guimera (Mgn), F. Guillemot (Mash1), J.F. Brunnet (Phox2a), H. Rhorer (DBH), B. Zalc (PLP-DM20), and finally to C. Soula (Sulf1) for providing the necessary plasmids used in the ISH probes. QT6 control and SHH-expressing QT6 cell lines were kindly provided by D. Duprez.

REFERENCES

Agarwala S, Ragsdale CW. 2002. A role for midbrain arcs in nucleogenesis. Development 129:5779–5788.

Agarwala S, Sanders TA, Ragsdale CW. 2001. Sonic hedgehog control of size and sharpe in midbrain pattern formation. Science 291:2147–2150.

Armelin HA. 1973. Pituitary and steroid hormones in the control of 3T3 cell growth. Proc Natl Acad Sci U S A 70: 2702–2706.

Barth KA, Wilson SW. 1995. Expression of zebrafish nk2.2 is influenced by sonic hedgehog/vertebrate hedgehog-1 and demarcates a zone of neuronal differentiation in the embryonic forebrain. Development 121:1755–1768.

Bellairs R, Osmond M. 1998. The atlas of chick development. New York: Academic Press.

Cambronero F, Puelles L. 2000. Rostrocaudal nuclear relationships in the avian medulla oblongata: a fate map with quail chick chimeras. J Comp Neurol 427:522–545.

Chi CL, Martinez S, Wolfgang W, Martin GR. 2003. The isthmic organizer signal FGF8 is required for cell survival in the prospective midbrain and cerebellum. Development 130:2633–2644.

Crossley PH, Martin GR. 1995. The mouse Fgf8 gene encodes a family of polypeptides and is expressed in regions that direct outgrowth and patterning in the developing embryo. Development 121: 439–451.

Crossley PH, Martinez S, Martin GR. 1996. Midbrain development induced by FGF8 in the chick embryo. Nature 380:66–68.

Duprez DM, Kostakopoulou K, Francis-West PH, Tickle C, Brickell PM. 1996. Activation of *Fgf-4* and *HoxD* gene expression by BMP-2 expressing cells in the developing chick limb. Development 122:1821–1828.

Easter SS, Ross LS, Frankfurter A. 1993. Initial tract formation in the mouse brain. J Neurosci 13:285–299.

Echevarria D, Vieira C, Martinez S. 2001. Mammalian neural tube grafting experiments: an in vitro system for mouse experimental embryology. Int J Dev Biol 45:895–902.

Echevarria D, Vieira C, Gimeno L, Martinez S. 2003. Neuroepithelial secondary organizers and cell fate specification in the developing brain. Brain Res Brain Res Rev 43:179–191.

Echevarria D, Martinez S, Marques S, Lucas-Teixeira V, Belo JA. 2005a. Mkp3 is a negative feedback modulator of FGF8 signaling in the mammalian Isthmic organizer. Dev Biol 284:351–363.

Echevarria D, Belo JA, Martinez S. 2005b. Modulation of Fgf8 activity during vertebrate brain development. Brain Res Rev 49:150–157.

Ericson J, Muhr J, Placzek M, Lints T, Jessell TM, Edlund T. 1995. Sonic hedgehog induces the differentiation of ventral forebrain neurons: a common signal for ventral patterning within the neural tube. Cell 81:747–756.

Garcia-Lopez R, Vieira C, Echevarria D, Martinez S. 2004. Fate map o the diencephalon and the zona limitans at the 10-somites stage in chick embryos. Dev Biol 268:514–530.

Garda A-L, Echevarria D, Martinez S. 2001. Neuroepithelial co-expression of *Gbx2* and *Otx2* precedes *Fgf8* expression in the isthmic organizer. Mech Dev 101: 111–118.

Gimeno L, Hashemi R, Brulet P, Martinez S. 2002. Analysis of *Fgf15* expression pattern in the mouse neural tube. Brain Res Bull 57:297–299.

Gimeno L, Brulet P, Martinez S. 2003. Study of *Fgf15* expression in developing mouse brain. Gene Expr Patterns 3:473–481.

Goldfarb M. 1996. Functions of fibroblast growth factors in vertebrate development. Cytokine Growth Factor Rev 7:311–325.

Graham A. 2000. Hear, hear, for the inner ear. Science 290:1904–1905.

Guillemot F, Joyner AL. 1993. Dynamic expression of the murine Achaete-Scute homologue Mash-1 in the developing nervous system. Mech Dev 42:171–185.

Guimera J, Vogt Weisenhorn D, Echevarria D, Martinez S, Wurst W. 2006. Molecular characterization, structure and developmental expression of Megane bHLH factor. Gene 377:65–76.

Hamburger H, Hamilton HL. 1951. A series of normal stages in the development of the chick embryos. J Morphol 88:49–92.

Ishibashi M, McMahon AP. 2002. A sonic hedgehog-dependent signalling relay regulates growth of diencephalic and mesencephalic primordia in the early mouse embryo. Development 129:4807–4819.

Ishibashi M, Saitsu H, Komada M, Shiota K. 2005. Signalling cascade coordinating growth of dorsal and ventral tissues of the vertebrate brain, with special reference to the involvement of Sonic hedgehog signalling. Anat Sci Int 80:30–36.

Itoh N, Ornitz DM. 2004. Evolution of the *Fgf* and *Fgfr* gene families. Trends Genet 20:563–569.

Joyner AL, Liu A, Millet S. 2000. *Otx2*, *Gbx2* and *Fgf8* interact to position and maintain a mid-hindbrain organizer. Curr Opin Cell Biol 12:736–741.

Katoh M. 2002. WNT and FGF gene clusters [Review]. Int J Oncol 21:1269–1273.

Katoh M, Katoh M. 2003. Evolutionary conservation of *CCND1-ORAOV1-FGF19-FGF4* locus from zebrafish to human. Int J Mol Med 12:45–50.

Kaufman MH. 1999. The atlas of mouse development. New York: Academic Press.

Kurose H, Bito T, Adachi T, Shimizu M, Noji S, Ohuchi H. 2004. Expression of Fibroblast growth factor 19 (*Fgf19*) during chick embryogenesis and eye development, compared with *Fgf15* expression in the mouse. Gene Expr Patterns 4:687–693.

Kurose H, Okamoto M, Shimizu M, Bito T, Marcelle C, Noji S, Ohuchi H. 2005. FGF19-FGFR4 signaling elaborates lens induction with the FGF8-L-Maf cascade in the chick embryo. Dev Growth Differ 47:213–223.

Ladher RK, Anakwe KU, Gurney AL, Schoenwolf GC, Francis-West PH. 2000. Identification of synergistic signals initiating inner ear development. Science 290: 1965–1967.

Ladher RK, Wright TJ, Moon AM, Mansour SL, Schoenwolf GC. 2005. FGF8 indicates inner ear induction in chick development. Genes Dev 19:603–613.

Leger S, Brand M. 2002. Fgf8 and Fgf3 are required for zebrafish ear placode induction, maintenance and inner ear patterning. Mech Dev 119:91–108.

Mahmood R, Kiefer P, Guthrie S, Dickson C, Mason I. 1995. Multiples roles for FGF-3 during cranial neural development in the chicken. Development 121: 1399–1410.

Marin F, Puelles L. 1995. Morphological fate of rhombomeres in quail/chick chimeras: a segmental analysis of hindbrain nuclei. Eur J Neurosci 7:1714–1738.

Maroon H, Walshe J, Mahmood R, Kiefer P, Dickson C, Mason I. 2002. Fgf3 and Fgf8 are required together for formation of the otic placode and vesicle. Development 129:2099–2108.

Martin GR. 1998. The roles of FGFs in the early development of vertebrate limbs. Genes Dev 12:1571–1586.

Martinez S. 2001. The isthmic organizer and brain regionalization. Int J Dev Biol 45:367–371.

Martinez S, Geijo E, Sanchez-Vives MV, Puelles L, Gallego R. 1992. Reduced junctional permeability at interrhombomeric boundaries. Development 116: 1069–1076.

Martinez S, Crossley PH, Cobos I, Rubenstein JLR, Martin GR. 1999. FGF-8 induces an isthmic organizer and isthmocerebellar development in the caudal forebrain via a repressive effect on Otx2 expression. Development 126:1189–1200.

Miyake A, Nakayama Y, Konishi M, Itoh N. 2005. Fgf19 regulated by Hh signalling is required for zebrafish forebrain development. Dev Biol 288:259–275.

Nishimura T, Utsunomiya Y, Hoshikawa M, Ohuchi H, Itoh N. 1999. Structure and expression of a novel human FGF, FGF-19, expressed in the fetal brain. Biochim Biophys Acta 1444:148–151.

Ornitz DM, Itoh N. 2001. Fibroblast growth factors. Genom Biol 2:REVIEW3005.

Ornitz DM, Xu J, Colvin JS, McEwen DG, MacArthur CA, Coulier F, Gao G, Goldfarb M. 1996. Receptor specificity of the fibroblast growth factor family. J Biol Chem 271:15292–15297.

Perez-Villegas EM, Olivier C, Spassky N, Poncet C, Cochard P, Zalc B, Thomas JL, Martinez S. 1999. Early specification of oligodendrocytes in the chick embryonic brain. Dev Biol 216:98–113.

Powers CJ, McLeskey SW, Wellstein A. 2000. Fibroblast growth factors, their receptor and signalling. Endocr Relat Cancer 7:165–197.

Puelles E. 2000. Patron de Expression Geneica e Histogenesis en la Placa Basal del Prosencefalo y Mesencefalo de Aves. Doctoral thesis Univ. Muricia, Spain.

Puelles E, Annino A, Tuorto F, Usiello A, Acampora D, Czerny T, Brodski C, Ang SL, Wurst W, Simeone A. 2004. Otx2 regulates the extent, identity and fate of neuronal progenitor domains in the ventral midbrain. Development 131:2037–2048.

Represa J, Leon Y, Iner C, Giraldez F. 1991. The int-2 proto-oncogene is responsible for induction of the inner ear. Nature 353:561–563.

Roessler E, Belloni E, Gaudenz K, Jay P, Berta P, Scherer SW, Tsui LC, Muenke M. 1996. Mutations in the human Sonic Hedgehog gene cause holoprosencephaly. Nat Genet 14:357–360.

Rubenstein JLR, Shimamura K, Martinez S, Puelles L. 1998. Regionalization of the prosencephalic neural plate. Annu Rev Neurosci 21:445–478.

Saitsu H, Komada M, Suzuki M, Nakayama R, Motoyama J, Shiota K, Ishi-

bashi M. 2005. Expression of the mouse Fgf15 gene is directly initiated by Sonic Hedgehog signaling in the diencephalon and midbrain. Dev Dyn 232:282–292.

Saitsu H, Shiota K, Ishibashi M. 2006. Analysis of Fibroblast growth factor 15 cis-elements reveals two conserved enhancers which are closely related to cardiac outflow tract development. Mech Dev 123:665–673.

Sanchez-Calderon H, Francisco-Morcillo J, Martin-Partido G, Hidalgo-Sanchez M. 2006. Fgf19 expression patterns in the developing chick inner ear. Gene Expr Patterns 7:30–38.

Sanders TA, Lumsden A, Ragsdale W. 2002. Arcuate plan of chick midbrain development. J Neurosci 22:10742–10750.

Schell-Apacik C, Rivero M, Knepper J, Roessler E, Muenke M, Ming JE. 2003. Sonic Hedgehog mutations causing holoprosencephaly impair neural patterning activity. Hum Genet 113:170–177.

Schubert FR, Lumsden A. 2005. Transcriptional control of early tract formation in the embryonic chick midbrain. Development 132:1785–1793.

Shimamura K, Rubenstein JLR. 1997. Inductive interactions direct early regionalization of the mouse forebrain. Development 124:2709–2718.

Shimamura K, Hirano S, McMahon AP, Takeichi M. 1994. Wnt-1-dependent regulation of local E-cadherin and aN-catenin expression in the embryonic mouse brain. Development 120:2225–2234.

Shimamura K, Hartigan DJ, Martinez S, Puelles L, Rubenstein JLR. 1995. Longitudinal organization of the anterior neural plate and neural tube. Development 121:3923–3933.

Storm EE, Garel S, Borello U, Hebert JM, Martinez S, McConnell SK, Martin GR, Rubenstein JLR. 2006. Dose-dependent functions of *Fgf8* in regulating telencephalic patterning centres. Development 133:1831–1844.

Thomas JL, Spassky N, Perez-Villegas EM, Olivier C, Cobos I, Goujet-Zalc C, Martinez S, Zalc B. 2000. Spatiotemporal development of oligodendrocytes in the embryonic brain. J Neurosci Res 59: 471–476.

Vieira C, Martinez S. 2005. Experimental study of MAP kinase phosphatase-3 (Mkp3) expression in the chick neural tube in relation to Fgf8 activity. Brain Res Rev 49:158–166.

Vieira C, Martinez S. 2006. Sonic Hedgehog signal from the basal plate and the zona limitans intrathalamica exhibits differential activity on diencephalic molecular regionalization and nuclear structure. Neuroscience 143:129–140.

Watanabe Y, Nakamura H. 2000. Control of chick tectum along dorsoventral axis by Sonic hedgehog. Development 127: 1131–1140.

Wright TJ, Mansour SL. 2003. Fgf3 and Fgf10 are required for mouse otic placode induction. Development 130:3379–3390.

Wright TJ, Ladher R, McWhirter JM, Murre C, Schoenwolf GC, Mansour SL. 2004. Mouse FGF15 is the ortholog of human and chick FGF19, but is not uniquely required for otic induction. Dev Biol 269:264–275.

Yamada T, Placzek M, Tanaka H, Dodd J, Jessell TM. 1991. Control of cell pattern in the developing nervous system: polarizing activity of the floor plate and notochord. Cell 64:635–647.